Palaeogeography, Palaeoclimatology, Palaeoecology 284 (2009) 120–128

Contents lists available at ScienceDirect

Palaeogeography, Palaeoclimatology, Palaeoecology

journal homepage: www.elsevier.com/locate/palaeo

Mid-Pliocene to Recent abyssal current flow along the Antarctic Peninsula: Results from ODP Leg 178, Site 1101

N.J.C. Hassold *, D.K. Rea, B.A. van der Pluijm, J.M. Parés

Department of Geological Sciences, University of Michigan, Ann Arbor, Michigan, United States

A R T I C L E I N F O

Article history:
Received 22 May 2008
Received in revised form 21 August 2009
Accepted 3 September 2009
Available online 30 September 2009

Keywords:
Antarctic Peninsula
Ocean current
Anisotropy of magnetic susceptibility
ODP Leg 178
Paleoclimatology

A B S T R A C T

Sediments recovered from a drift deposit located on the Pacific side of the Antarctic Peninsula (ODP Leg 178, Site 1101) give a physical record of a bottom current, sourced from the Weddell Sea Deep Water, for the past 3 Ma. Sediment grain size and magnetic fabric analyses indicate a contourite depositional environment and little change in the average intensity of this current. Terrigenous fluxes decreased around the time of the onset of Northern Hemisphere Glaciation, which we interpret as a freezing of the base of the Antarctic Peninsula Ice Cap. Terrigenous fluxes have increased since 1.7 Ma implying a possible return of the Antarctic Peninsula Ice Cap to a more wet-based ice sheet.

1. Introduction

The Southern Ocean is the vital connection among the Atlantic, Pacific and Indian oceans (Wright et al., 1991; Pudsey and Howe, 1998; Barker and Thomas, 2004; van de Flierdt et al., 2004). As the source of Antarctic Bottom Water (AABW), the deepest of the water masses, it is a crucial aspect of the global environment (Wright et al., 1991; Pudsey and Howe, 1998). Here North Atlantic Deep Water (NADW) mixes with AABW to form Circumpolar Deep Water (CDW), a water mass which is divided into two masses: the Upper Circumpolar Deep Water (UCDW) and the Lower Circumpolar Deep Water (LCDW) (Orsi et al., 1995). These water masses circulate around the Antarctic continent, splitting off at various depths to flow north into the other ocean basins, completing the deep ocean portion of the circulation circuit and resulting in a transfer of heat, salt and nutrients around the globe.

The Antarctic Circumpolar Current (ACC) is a globe-circling, wind-driven current that extends from the surface to the sea floor along most of its path (Orsi et al., 1995; Camerlenghi et al., 1997a; van de Flierdt et al., 2004) and transports UCDW, LCDW and various surface and intermediate waters eastward, linking all oceans. It is defined as occurring between the Subtropical Front (STF) in the north and the Polar Front (PF) in the south (Orsi et al., 1995) although the STF is not continuous in Drake Passage. The ACC is the strongest current in the world, having a volumetric transport of ~137 ± 8 Sv (1 Sv = 10^6 m^3/s) (Cunningham et al., 2003), most of which is carried by two jets within the current (Naveira Garabato et al., 2004). Creation of the modern ACC began after Drake Passage opened, probably in the Oligocene although there is still debate on the exact time, with modern current strength likely established by late Oligocene (Barker and Burrell, 1977; Lawver and Gahagan, 2003; Pfuhl and McCave, 2005; Lyle et al., 2007).

Along the western AP, the ACC dominates the upper water column, flowing along the shelf slope break. At other locations around the continent, the southern boundary of the ACC is offshore of the shelf (Cunningham et al., 2003). South of the Polar Front is the subpolar regime. In this region, along the Pacific margin of the Antarctic Peninsula, a southwestward flowing bottom current (Barker and Thomas, 2004; Camerlenghi et al., 1997b; Pudsey, 2001) which follows the bathymetric contours along the continental shelf and slope, affects the sediment drifts. Parés et al. (2007) confirm this direction for flow over the past 3 Ma (2007). Hillenbrand et al. (2008) suggest the source of this current is modified Weddell Sea Deep Water (WSDW). Further as flow patterns of this current may mimic those of the ACC, these Antarctic Peninsula drifts may allow inferences to the history of the circumpolar flow (Camerlenghi et al., 1997a).

Deep-sea currents carrying sediments deposit them along the slopes of topographical highs on the ocean bottom. The resulting sediment drifts are associated with many deep currents and can yield high-resolution records of paleoceanographic phenomena (Kidd and Hill, 1987; Hall et al., 2001; Joseph et al., 2002; 2004; Hassold et al., 2006, 2009). Several sediment drifts are located along the Pacific Margin of the Antarctic Peninsula continental rise, providing an

* Corresponding author. Current address: Earth and Resource Science Department, University of Michigan-Flint, 303 E. Kearsley Street, Flint MI, United States.
E-mail address: nhassold@umflint.edu (N.J.C. Hassold).

0031-0182/$ – see front matter © 2009 Elsevier B.V. All rights reserved.
doi:10.1016/j.palaeo.2009.09.011

opportunity to study the effects of climate change on the bottom current and the WSDW.

These drifts are built from sediments eroded from the Antarctic Peninsula and transported to the shelf edge by grounding events of the ice sheet, where, as the ice sheet recedes and sea level rises, they are carried down slope in turbidity currents and then transported to the southwest by the Antarctic Counter Current (Camerlenghi et al., 1997a) along the Antarctic continental rise and the adjoining sea floor (Maldonado et al., 2003; 2005). Many researchers have studied these and other sediment drifts to understand changes in current strength and climate using a variety of methods, including anisotropy of magnetic susceptibility (AMS), grain size distribution or both (for example, see Ellwood and Ledbetter, 1977; Ellwood et al., 1979; Ledbetter, 1979, 1984; Joseph et al., 1998; 2002; McCave et al., 1995; Parés et al., 2007; Hassold et al., 2009).

Here we present results from a study using anisotropy of magnetic susceptibility and grain size data to determine the relative strength of bottom currents along the Antarctic Peninsula since the late Pliocene. We also use the mass accumulation rate (MAR) of opal and terrigenous sediments as evidence of sea surface and land conditions, respectively. Of particular interest is which of these data sets, if any, may reflect the onset and later intensification of Northern Hemisphere Glaciation.

2. Geological setting

Ocean Drilling Program (ODP) Leg 178 drilled at several locations along the Pacific margin of the Antarctic Peninsula. Site 1101 (latitude 64° 22.3′S, longitude 70° 15.6′W, 3280 m) is located on Drift 4, one in a series of eight drift deposits that occur along the northwest flank of the Antarctic Peninsula continental rise (Fig. 1; Barker et al., 1999; Uenzelmann-Neben, 2006). Drilling at this part of the margin provided a nearly continuous record of the past 3 million years that records the influence of drift-current flow offshore from the climatically sensitive Antarctic Peninsula Ice Cap (APIC) (Bart and Anderson, 2000; Anderson et al., 2002).

Site 1101 was drilled to 217.7 m below sea floor (mbsf) and recovered clayey and siliceous silts, foram-bearing clay and diatom ooze ranging in age from late Pliocene through Pleistocene. This site was single-cored and so a truly continuous section could not be constructed, nevertheless Site 1101 currently provides the best available record of Southern Ocean deposition over the past 3 Ma.

3. Methods

3.1. Ages and age models

The paleomagnetic data from Acton et al. (2002) and the geomagnetic polarity time scale of Cande and Kent (1995) are the basis for the age model used in this study, from which the linear sedimentation rates (LSRs) were calculated (Fig. 2, Supplemental Table 1). As seen in Fig. 2, the linear sedimentation rates are not constant throughout the core; between 1.7 and 2.0 Ma the LSR decreases by a factor of 2.

3.2. Sediment component determination

One hundred thirty-two sediment samples were taken from cores 1H through 24X, with a resulting sampling interval of 20 ka to 30 ka. Obvious turbidites were avoided during the sampling. Several samples from the top of the core were not used in the analyses due to coring disturbance. Approximately 1 g of each sample was weighed, freeze-dried, reweighed and chemically treated using the mineral extraction method of Rea and Janecek (1981) and as modified by Hovan (1995) to isolate the terrigenous fraction. This procedure removes $CaCO_3$, oxides and hydroxides, and biogenic opal. After removal of the $CaCO_3$ and oxides and hydroxides, but prior to opal removal, the samples were sieved to remove the >63 µm fraction. This fraction was dried and weighed to determine its weight percent. After opal removal, the samples were again freeze-dried and weighed. Coarse mineral grains captured on the 63 µm screen are considered in this study to be ice-rafted debris. The weight percent terrigenous component and, by difference in these 2-component sediments, weight percent SiO_2 were calculated. Weight percentage values are accurate to ±3% of the values.

3.3. Mass accumulation rates

Mass accumulation rates (MAR) are a measure of the supply of sediment to the drift. MARs calculated using LSRs determined for this study and the dry bulk densities measured by the Shipboard Scientific Party (Rea and Janecek, 1981; Barker et al., 1999). The sediment component MARs were calculated using the % component and the flux:

$$MAR\,component(\mathrm{g/cm^2/ka}) = LSR(\mathrm{cm/ka}) \times DBD(\mathrm{g/cm^3}) \times \%component.$$

Mass accumulation rates provide a more accurate picture of deposition than do relative abundance data, as the effects of dilution by other components and of downcore compaction are eliminated.

3.4. Grain size analysis

Grain size distributions of the <63 µm fraction were determined using a Coulter Multisizer III. Joseph et al. (1998) have shown that the resulting distribution reflects the depositional environment. Drift and hemipelagic sediments both show a low, broad grain-size distribution (see Rea and Hovan, 1995; Joseph et al., 1998). Median grain size values (φ_{50}) were calculated for samples that were not turbidites or disturbed by coring, where $\varphi = -\log_2$(diameter mm). The standard deviation of φ_{50} is 0.1φ.

3.5. Magnetic susceptibility

Two hundred eighty-one 8 cm^3 samples in plastic cubes were taken for rock magnetic analysis, resulting in a sampling interval of about 11 ka. Samples from cores 1H through 15H, excluding core 5H, which was not available, were taken from pre-existing U-channel samples, while samples from cores 16H through 24X were taken from the working half of the Site 1101 core by the ODP Bremen Repository staff. Samples from sections with obvious drilling disturbance were not used in this study.

Anisotropy of Magnetic Susceptibility (AMS) analyses were carried out on a Kappabridge KLY-2.03 susceptibility bridge (AGICO) at the University of Michigan, which measures the magnetic susceptibility of the sample in 15 different directions, in order to determine the magnetic susceptibility ellipsoid. The AMS ellipsoid can be defined by its three principal axes of magnetic susceptibility: maximum (K_{max}), intermediate (K_{int}), and minimum (K_{min}). Previous laboratory studies have determined that the distribution of the AMS axes reflects the depositional plane (Rees and Woodall, 1975; Tarling and Hrouda, 1993) for sediments. We therefore assume the orientation of the ellipsoid to reflect the depositional environment of the sediments. The anisotropy parameter P' is determined mathematically from the directional susceptibility measurements, and is a measure of the degree of anisotropy of magnetic susceptibility ellipsoid. The parameter T, also determined mathematically, is a measure of the shape of the ellipsoid, whether oblate ($0 < T \leq 1$) or prolate ($-1 \leq T < 0$) (Tarling and Hrouda, 1993).

Low field magnetic susceptibility in sediments results from the total contribution of its bulk mineralogy. In terrigenous sediments, the magnetic fabric is directly related to the preferred orientation of

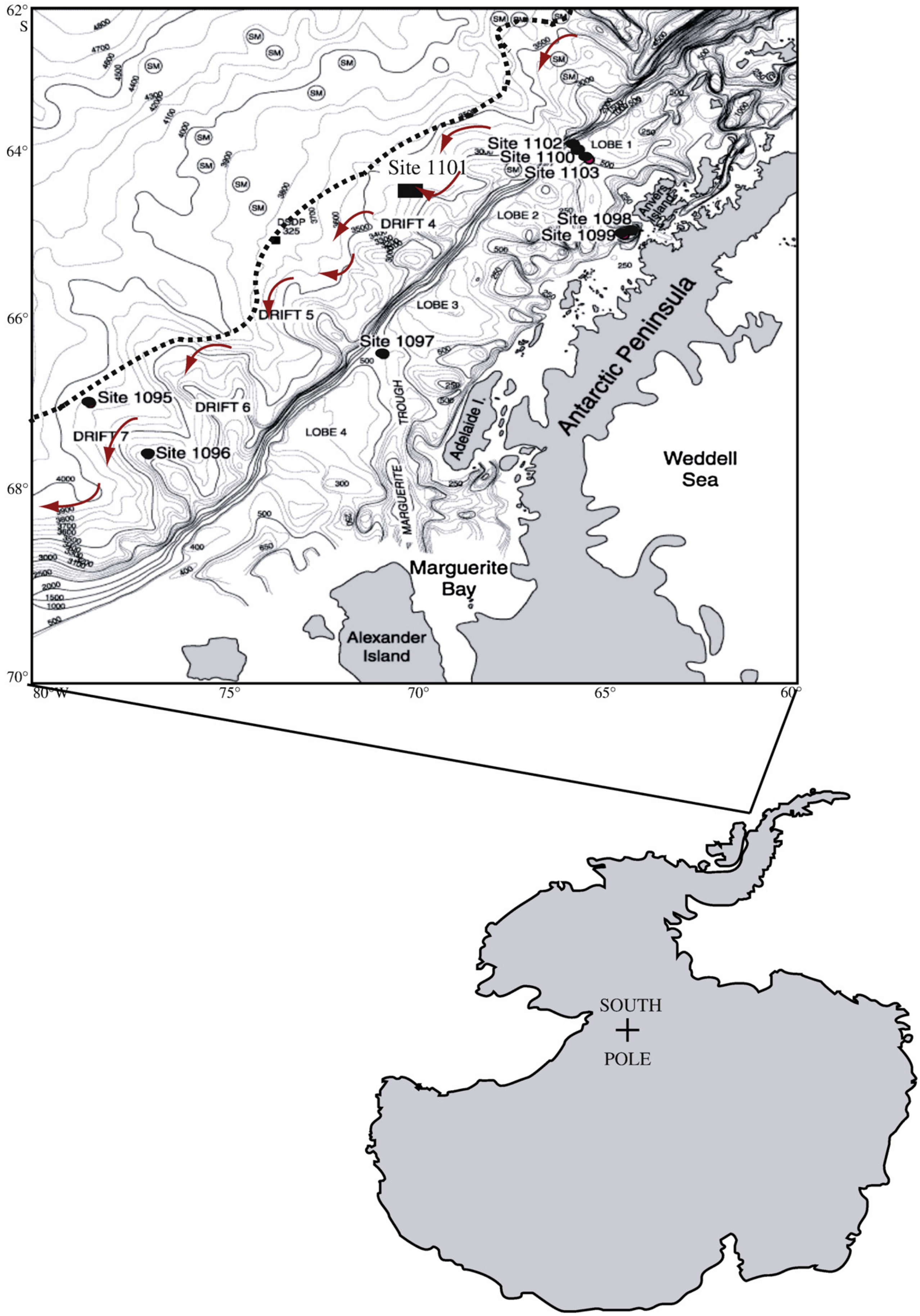
62° S
64°
66°
68°
70°
80° W
75°
70°
65°
60°
Site 1102
Site 1100
Site 1103
Site 1101
LOBE 1
LOBE 2
LOBE 3
LOBE 4
Site 1098
Site 1099
Anvers Island
DRIFT 4
DRIFT 5
DRIFT 6
DRIFT 7
DSDP 325
Site 1097
Site 1095
Site 1096
TROUGH
MARGUERITE
Adelaide I.
Antarctic Peninsula
Weddell Sea
Marguerite Bay
Alexander Island
SM
SOUTH
POLE

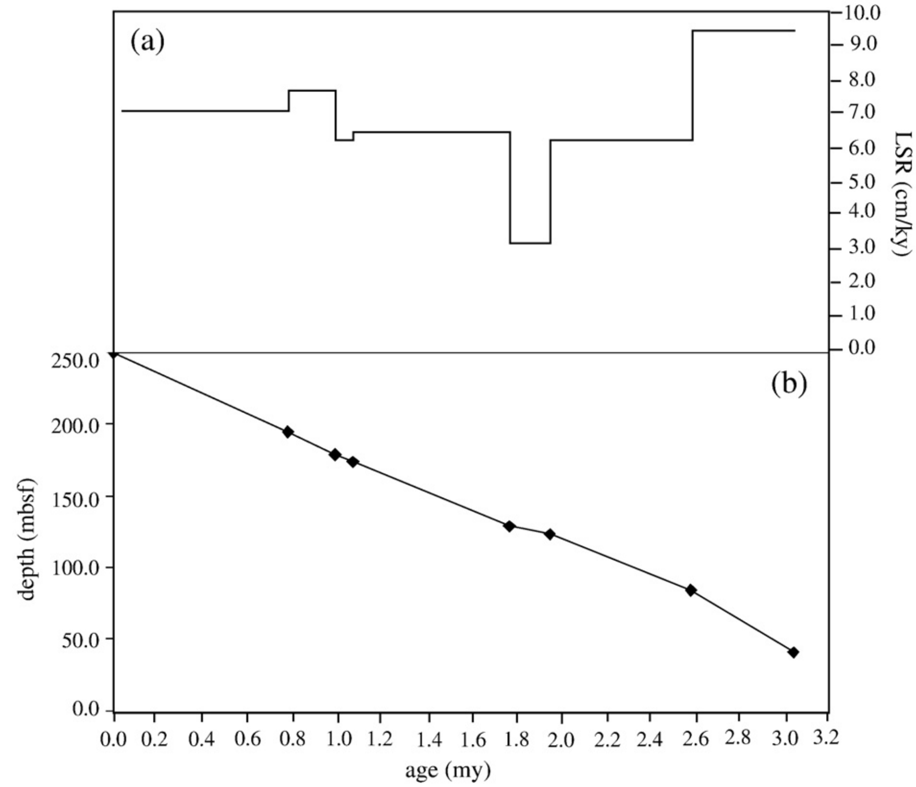

Fig. 2. Age model plot for Site 1101.

the sediment grains, which are generally phyllosilicates in the studied sediments, and processes that affect grain orientation will determine the fabric, with K_{min} generally perpendicular to and K_{max} and K_{int} parallel to the bedding plane (e.g. Parés et al., 2007). Previous studies (Ellwood and Ledbetter, 1977,1979; Ledbetter and Ellwood, 1980) have shown that magnetic fabric analysis provides a method for determining relative current strengths; strong currents will align grains while environments with little or no current will result in a more random grain alignment and hence lower degree of anisotropy, *P*. More recent work by Joseph et al. (1998; 2002) showed that combining AMS and grain size distribution data provides a robust method for determining depositional environments.

To determine the magnetic mineral characteristics, selected samples were immersed in liquid nitrogen for 30 min and then the bulk susceptibility was measured periodically as the sample warmed to room temperature (Parés and van der Pluijm, 2002; Richter and van der Pluijm, 1994). The ratio of room to liquid nitrogen temperature susceptibility is an indicator of the relative amounts of phyllosilicates. Following this analysis, saturation isothermal remanent magnetization (sIRM) measurements (using a 2G Enterprises cryogenic magnetometer house in a field-free room at the University of Michigan) were carried out on these samples. These are tests to determine whether the magnetic susceptibility is dominantly carried by ferrimagnetic or paramagnetic, i.e. phyllosilicate, phases.

4. Results

Average grain size of the terrigenous component is 6.8 φ (9 μm), with a range between 6.1 φ and 7.3 φ (15–6.2 μm) and a mode of 6.9 φ (8.3 μm) (Fig. 3a, Supplemental Table 2). The variation in size is consistent with what would be expected from a contourite current moving sediment originating in flows down the continental slope. Joseph et al. (1998) found turbidite φ_{50} values between 5.1 φ and 6.8 φ (29–9 μm) for samples from the Delgada Fan, and drift φ_{50} values of 6.2 φ to 6.8 φ (13.5–8.9 μm) for the Blake Outer Ridge sediment drift deposits. At Kerguelen, Joseph et al (2002) determined a median terrigenous grain size range of 6.2 φ to 7.5 φ (13.6–5.5 μm) for samples from the Kerguelen drift.

The weight percent terrigenous and silica components remained fairly constant back to about 2.0 Ma, 67% for the terrigenous component and 32% for the silica component (Fig. 3b; Supplemental Table 2). Between 2 Ma and 2.6 Ma, the % terrigenous component decreased to an average of 58%, the silica increased to 41%, and remained at these approximate levels to the bottom of the record.

Mass accumulation rates were quite high, and ranged between 3.6 g/cm^2 ka and 10.8 g/cm^2 ka for the terrigenous component and 1.3 g/cm^2 ka and 9.9 g/cm^2 ka for the opal component (Fig. 3c; Supplemental Table 2). From 0 to 1.8 Ma, the terrigenous and silica MAR averaged 8.2 g/cm^2 ka and 3.9 g/cm^2 ka, respectively. Between 1.8 Ma and 2.0 Ma, there was a large decrease in MAR, following a decrease in the LSR, for both components. Between 2.0 Ma and 2.6 Ma, the average MAR was higher than 1.8 Ma for the silica (4.5 g/cm^2 ka vs 3.9 g/cm^2 ka). For the terrigenous components, the average at this time was 6.3 g/cm^2 ka. For sediments older than 2.6 Ma, there was a jump to 9 g/cm^2 ka for the terrigenous and 7 g/cm^2 ka for silica.

Bulk susceptibility increased from 0 to 0.45 Ma and remained fairly constant to 1.7 Ma (Fig. 4a, Supplemental Table 3). A slight decrease

Fig. 1. Map of Antarctica, showing the location of Site 1101. The dotted line represents the southern ACC, the red arrows show the path of the current along the continental slope (after Uenzelmann-Neben, 2006). (For interpretation of the references to color in this figure legend, the reader is referred to the web version of this article.)

occurred between 1.7 and 2.2 Ma. An increase occurred between 2.2 and 2.5 Ma, followed by a decrease to 3.1 Ma. Magnetic fabric strength (P') remained fairly constant (Fig. 4b, Supplemental Table 3), with an average value of 1.07 with a standard deviation of 0.04 (Supplemental Tables 4 and 5). Averages computed from a range of ages have overlapping standard deviations, implying essentially no change in the P' values over time.

Cold temperature (liquid nitrogen) studies were carried out to determine if the mineralogy of the core changed through that interval. Several samples were cooled to 77 K and allowed to warm up to room temperature, while the susceptibility was measured every 30 s (Supplemental Table 6). Plots of the K_0/K ratio vs time are shown in Fig. 5. The bulk susceptibility at 77 K vs 298 K gives a linear plot which is shown in Fig. 6 (Supplemental Table 7). Saturation IRM data are given in Supplemental Table 8 and indicate no change in the magnetic fabric carrier of the sediments through the core.

Fig. 7 shows data from the present study plotted on the depositional fields developed by Joseph et al. (1998). These data are similar to those seen elsewhere with the drift-like grainsize distributions (Fig. 7a) and moderate to strong P' values (Fig. 7b) (Joseph et al., 1998, 2002; Hassold et al., 2009).

5. Paleoceanography and paleoclimatology

The large reduction in mass accumulation rates for the terrigenous and biogenic silica components at ~2.6 Ma occurred around the same time as the onset of Northern Hemisphere glaciation (Fig. 3c) (Hillenbrand and Ehrmann, 2005). The decrease in the terrigenous signal is most likely due to basal freezing of the APIC, resulting in less sub-glacial melting and erosion (Hallet et al., 1996). Rebesco et al. (2006) and Rebesco and Camerlenghi (2008) studied seismic images from the Antarctic Peninsula and other sites around the continental shelf of Antarctica and detected a regional

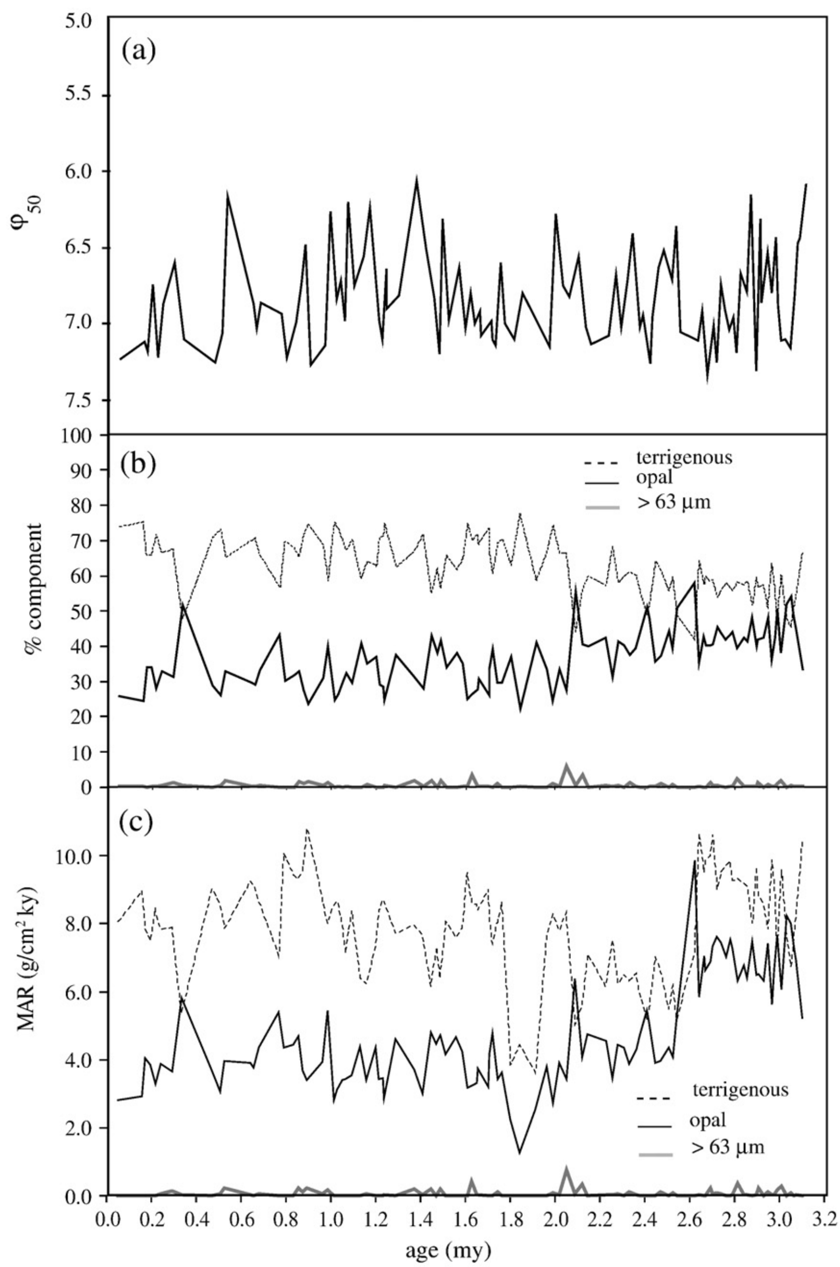

Fig. 3. Plots of the MAR, LSR and phi 50 values for Site 1101.

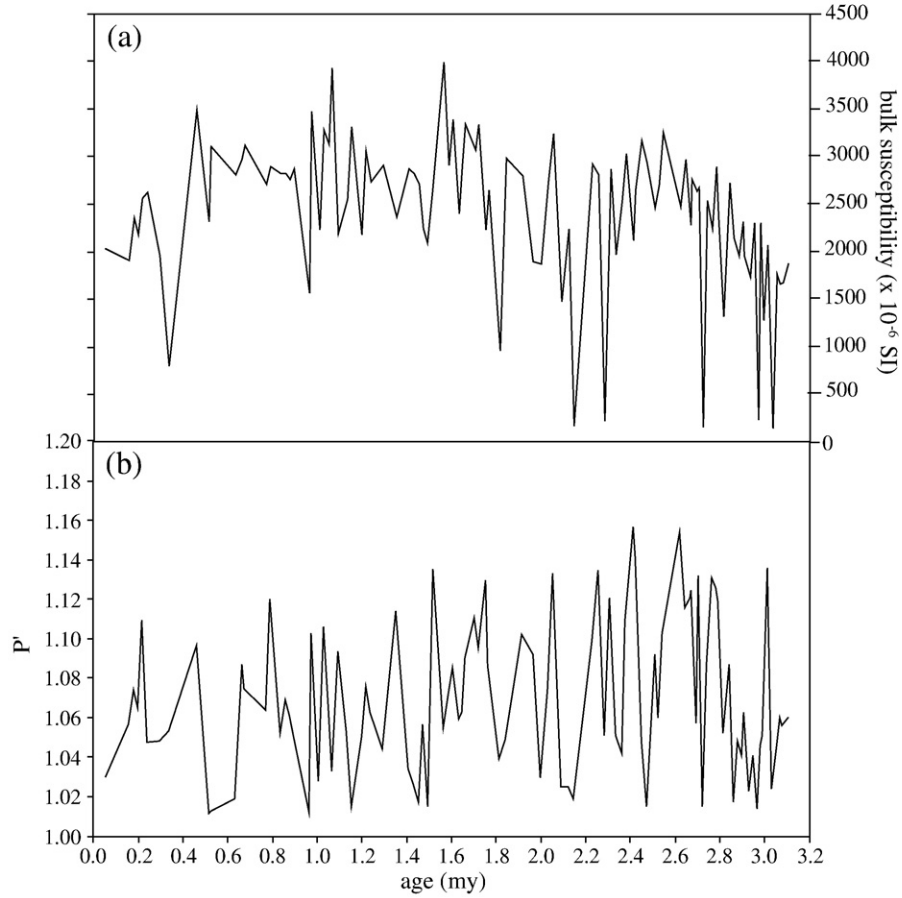

Fig. 4. Magnetic fabric and bulk susceptibility plots for Site 1101.

change in the sediment accretion at an approximate time of 3 Ma, which they relate to the transition to the modern Antarctic ice sheet, i.e., a cold-based ice sheet. Our sediment MAR data suggest an age of about 2.6 Ma for this transition on the Antarctic Peninsula. We also see an increase in terrigenous sediment accumulation 1.7 Ma, perhaps indicating a return to a more wet-based ice sheet.

The permanent decline in opal flux at 2.6 Ma has been seen by other researchers from sites around the globe (Froelich et al., 1991; Farrell et al., 1995; Rea and Snoeckx, 1995; Maslin et al., 1998; Sigman et al., 2004). Rea and Snoeckx (1995) reported a several-fold opal flux decrease in the northwest Pacific at 2.6 Ma. Cortese et al. (2004) studied patterns of global opal deposition over the past 15 m. y. and reported an opal deposition rate reduction in the Bellingshausan Sea between 3 Ma and 2.5 Ma. Hillenbrand and Fütterer (2000), Hillenbrand and Ehrmann (2005) and Hassold et al. (2009) noted the decrease in opal deposition that occurs between 3.1 Ma and 1.8 Ma at the Leg 178 drillsites, which they attributed to sea ice expansion. Our biogenic silica flux values at Site 1101 decrease by a factor of 2 (from 8 g/cm^2 ka to 4 g/cm^2 ka) at 2.6 Ma, in agreement with these other studies. Together, these studies in the North Pacific and the Southern Ocean all point to a marked reduction in oceanic biological productivity around the time of onset of Northern Hemisphere glaciation.

The terrigenous MAR gradual increase between 1.8 and 0.8 Ma is likely a result of numerous glacial–interglacial advances and retreats of the peninsular ice cap to the continental shelf edge. Cowen (2002) reports a large peak in the IRD at 1.9 Ma at Site 1101. We see a slight peak at ~1.6 Ma, but other larger peaks occur at ~2.0 Ma and ~0.10 Ma. Over the entire time span there are many peaks, implying numerous periods of glacial advance and retreat (Naish et al., 2009). This is in agreement with Bart and Anderson (2000), who observed 31 glacial unconformities in the seismic stratigraphy of the shelf around Marguerite Bay. These they attributed to grounding events of the APIC on the shelf and interpreted them as the minimum number of times the APIC had advanced and retreated during the late Neogene.

The new kind of information we bring to these studies is an estimate of current strength as indicated by the strength of the magnetic fabric, P' (Fig. 4b). The current strength is shown to vary uniformly throughout the record, with a minor gradual decreasing trend. The terrigenous component grainsize record behaves in a similar fashion (Fig. 3a) and supports the hypothesis of a modest variation around a constant average current.

Studies of ocean circulation have indicated that, in general, the deep ocean currents have slowed down during the later Cenozoic, as evidenced by changes in deposition on various sediment drifts, and polar regions have cooled (Wright et al., 1991; Raymo et al., 1992; Maslin et al., 1996; Rebesco et al., 1997; Frank et al., 2002; Kerr et al., 2005; Hassold et al., 2009). Pliocene reduction in deep water flow occurred at Feni and Gardar Drifts in the North Atlantic (Kidd and Hill, 1987; Hassold et al., 2006). Kerr et al. (2005) studied Meiji Drift on Detroit Seamount in the northwestern-most Pacific and determined that the current strength there has decreased since the Miocene. Joseph et al. (2002) detected a steady decrease in current strength since the late Miocene at Kerguelen Plateau in the Indian Ocean. Ravelo and Andreasen (2000) detected a relative decrease in the NADW flux between 3.0 and 2.5 Ma, which they attributed to climate cooling and Raymo et al. (1992) concluded that global cooling over the last 3 Ma resulted in a gradual decrease in the formation of NADW. Frank et al. (2002) studied the Nd and Pb isotopic signatures in ferromanganese crusts and suggest a strong export of NADW to the

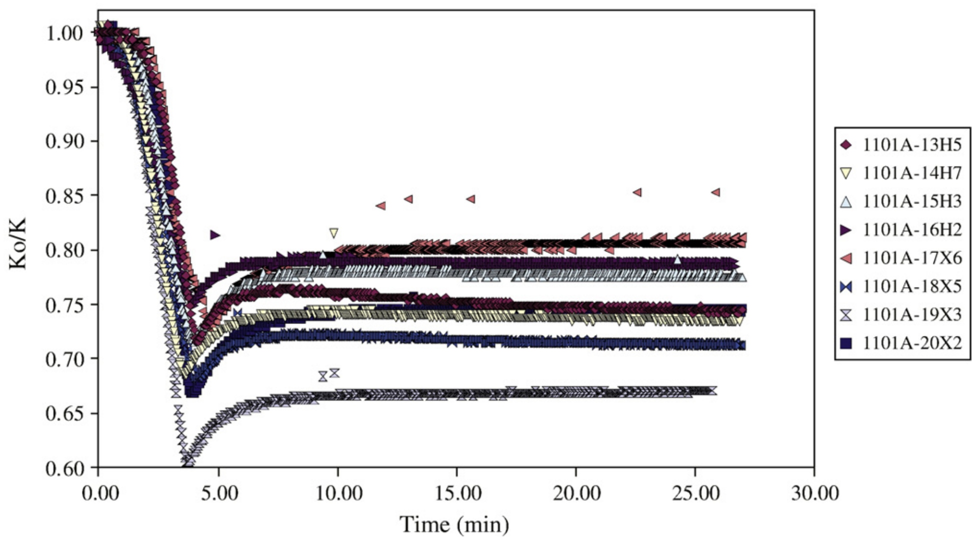

Fig. 5. Plots of the cold temperature study done on selected samples from Site 1101.

Southern Ocean between 14 and 3 Ma, but a reduction since the late Pliocene. Our present work on sediments from Site 1101 shows that during the last 3 m.y. the current along the Antarctic Peninsula, an outflow of Weddell Sea Deep Water, varied around a very slightly decreasing mean (Fig. 4b), in agreement with other researchers (Rebesco et al., 1997).

6. Summary

Sediments at Site 1101 are siliceous silts deposited by drift-current processes over the past 3 Ma. Grain size, in addition to the magnetic fabric data, indicate a drift depositional environment, as seen at Site 1095 (Fig. 7) (Camerlenghi et al., 1997a; 1997b; Parés et al., 2007; Hassold et al., 2009).

The physical methods employed in this study have given new insights into the behavior of the Antarctic Peninsula Ice Cap and the Weddell Sea Deep Water overflow at Site 1101 over the last 3 m.y. The degree of the anisotropy of magnetic susceptibility, a proxy for paleocurrents, has varied around a slightly decreasing mean, with no indication of significant changes at 0.8, 1.8, and 2.6 Ma. We interpret this as denoting no significant change in the current strength at Site 1101 for the past 3 m.y. Grain size analyses are also consistent with this interpretation, supporting our hypothesis that the ice volume and the Southern Ocean currents are not closely coupled in their response to climate changes.

Terrigenous sediment MAR decreases at 2.6 Ma, around the time of onset of major Northern Hemisphere Glaciation. This we interpret as the freezing of the base of the Antarctic Peninsula ice cap with a change in the efficacy of erosion and the type of sediment transport. Opal MAR decreases by a factor of 2 at 2.6 Ma, a decrease that is widely observed, and likely part of a global reduction in silica productivity at that time.

Acknowledgments

We would like to thank Walter Hale and the staff of the IODP Bremen Core Repository for assisting us in acquiring samples from ODP Site 1101. Marlon Jean assisted in the chemical isolation of the terrigenous fraction. This work was funded by the NSF Grant

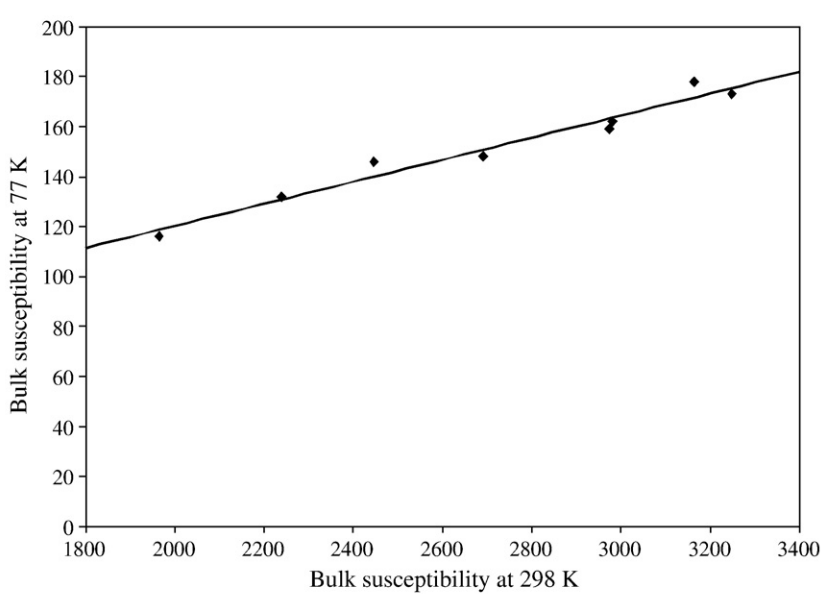

Fig. 6. Plot of bulk susceptibility at 298 K and 77 K showing the linear relationship.

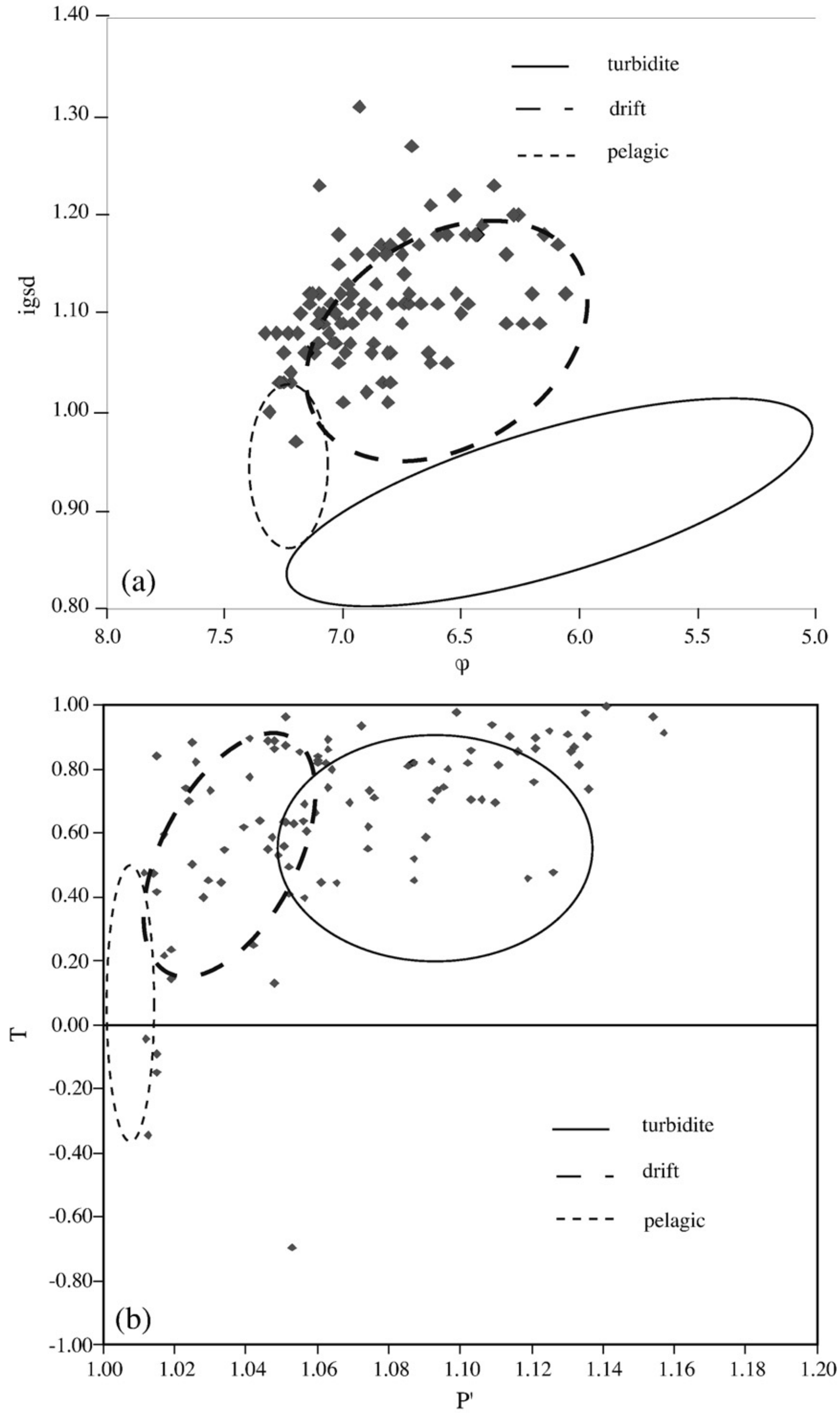

Fig. 7. Environmental plots for Site 1101 (based upon the plots developed by Joseph et al.) showing drift-like grain-size distributions (a.) and moderate to strong magnetic fabric strength (b.).

OPP-0337091. We thank two anonymous reviewers for their helpful comments.

Appendix A. Supplementary data

Supplementary data associated with this article can be found, in the online version, at doi:10.1016/j.palaeo.2009.09.011.

References

Acton, G.D., Guyodo, Y., Brachfeld, S.A., 2002. Magnetostratigraphy of sediment drifts on the continental rise of west Antarctica (ODP Leg 178, Sites 1095, 1096, and 1101). In: Barker, P.F., Camerlenghi, A., Acton, G.D., Ramsay, A.T.S. (Eds.), Proceedings of the Ocean Drilling Program ODP Scientific Results, 178, CD-ROM, pp. 1–61. Available from: Ocean Drilling Program, College Station, TX, 77845-9547, USA.

Anderson, J.B., Shipp, S.S., Lowe, A.L., Wellner, J.S., Mosola, A.B., 2002. The Antarctic Ice Sheet during the Last Glacial Maximum and its subsequent retreat history: a review. Quaternary Science Reviews 21, 49–70.

Barker, P.F., Burrell, J., 1977. The opening of Drake Passage. Marine Geology 25, 15–34.

Barker, P.F., Thomas, E., 2004. Origin, signature and palaeoclimatic influence of the Antarctic Circumpolar Current. Earth-Science Reviews 66, 143–162. doi:10.1016/j.earscirev.2003.10.003.

Barker, P.F., Camerlenghi, A., Acton, G.D., Party, S.S., 1999. Site 1101. In: Barker, P.F., Camerlenghi, A., Acton, G.D. (Eds.), Proceedings of the Ocean Drilling Program, Initial Reports, 178, CD-ROM, pp. 1–83. Available from: Ocean Drilling Program, College Station, TX, 77845-9547, USA.

Bart, P.J., Anderson, J.B., 2000. Relative temporal stability of the Antarctic ice sheets during the late Neogene based on the minimum frequency of outer shelf grounding events. Earth and Planetary Science Letters 182, 259–273.
Camerlenghi, A., et al., 1997a. Ten-month observation of the bottom current regime across a sediment drift of the Pacific margin of the Antarctic Peninsula. Antarctic Science 9 (4), 426–433.
Camerlenghi, A., Rebesco, M., Pudsey, C.J., 1997b. High resolution terrigenous sedimentary record of a sediment drift on the Antarctic Peninsula Pacific Margin (initial results of the 'SEDANO' program). The Antarctic Region: Geological Evolution and Processes, pp. 705–710.
Cande, S.C., Kent, C.V., 1995. Revised calibration of the geomagnetic polarity timescale for the Late Cretaceous and Cenozoic. Journal of Geophysical Research 100 (B4), 6093–6095.
Cortese, G., Gersonde, R., Hillenbrand, C.-D., Kuhn, G., 2004. Opal sedimentation shifts in the World Ocean over the last 15 Myr. Earth and Planetary Science Letters 224, 509–527.
Cowen, E.A., 2002. Identification of the glacial signal from the Antarctic Peninsula since 3.0 Ma at Site 1101 in a continental rise sediment drift. In: Barker, P.F., Camerlenghi, A., Acton, G.D., Ramsay, A.T.S. (Eds.), Proceedings of the Ocean Drilling Program, Scientific Results, 178, CD-ROM, pp. 1–22. Available from: Ocean Drilling Program, College Station, TX, 77845-9547, USA.
Cunningham, S.A., Alderson, S.G., King, B.A., Brandon, M.A., 2003. Transport and variability of the Antarctic Circumpolar Current in Drake Passage. Journal of Geophysical Research 108. doi:10.1029/2001JC001147.
Ellwood, B.B., Ledbetter, M.T., 1977. Antarctic bottom water fluctuations in the Vema Channel: effects of velocity changes on particle alignment and size. Earth and Planetary Science Letters 35, 189–198.
Ellwood, B.B., Ledbetter, M.T., 1979. Paleocurrent indicators in deep-sea sediment. Science 203, 1335–1337.
Ellwood, B.B., Ledbetter, M.T., Johnson, D.A., 1979. Sedimentary fabric: a tool to delineate a high-velocity zone within a deep western Indian Ocean bottom current. Marine Geology 33, M51–M55.
Farrell, J.W., et al., 1995. Late Neogene sedimentation patterns in the eastern equatorial Pacific Ocean. In: Pisias, N.G., Mayer, L.A., Janecek, T.R., Palmer-Julson, A., van Andel, T.H. (Eds.), Proceedings of the Ocean Drilling Program. Scientific Results. Leg 138, Ocean Drilling Program, College Station, TX, pp. 717–753.
Frank, M., Whiteley, N., Kasten, S., Hein, J.R., O'Nions, K., 2002. North Atlantic Deep Water export to the Southern Ocean over the past 14 Myr: evidence from Nd and Pb isotopes in ferromanganese crusts. Paleoceanography 17. doi:10.1029/2000PA000606.
Froelich, P.N., et al., 1991. Biogenic opal and carbonate accumulation rates in the subantarctic South Atlantic: the late Neogene of Meteor Rise Site 704. In: Ciesielski, P.F., Kristoffersen, Y., et al. (Eds.), Proceedings of the Ocean Drilling Program, Scientific Results. Ocean Drilling Program, College Station, TX, pp. 515–532.
Hall, I.R., McCave, I.N., Shackleton, N.J., Weedon, G.P., Harris, S.E., 2001. Intensified deep Pacific inflow and ventilation in Pleistocene glacial times. Nature 412, 809–812.
Hallet, B., Hunter, L., Bogen, R., 1996. Rates of erosion and sediment evacuation by glaciers: a review of field data and their implications. Global and Planetary Change 12, 213–235.
Hassold, N.J.C., et al., 2006. Late Miocene to Pleistocene paleoceanographic records from the Feni and Gardar Drifts: Pliocene reduction in abyssal flow. Palaeogeography, Palaeoclimatology, Palaeoecology 236, 290–301. doi:10.1016/j.palaeo.2005.11.011.
Hassold, N.J.C., Rea, D.K., van der Pluijm, B.A., Parés, J.M., 2009. A physical record of the Antarctic Circumpolar Current: Late Miocene to recent slowing of abyssal circulation. Palaeogeography, Palaeoclimatology, Palaeoecology 275, 28–36. doi:10.1016/j.palaeo.2009.01.011.
Hillenbrand, C.-D., et al., 2008. The present and past bottom-current flow regime around the sediment drifts on the continental rise west of the Antarctic Peninsula. Marine Geology 255, 55–63. doi:10.1016/j.margeo.2008.07.004.
Hillenbrand, C.-D., Fütterer, D.K., 2000. Neogene to Quaternary deposition of opal on the continental rise west of the Antarctic Peninsula, ODP Leg 178, Sites 1095, 1096, and 1101. In: Barker, P.F., Camerlenghi, A., Acton, G.D., Ramsay, A.T.S. (Eds.), Proceedings of the Ocean Drilling Program, Scientific Results, 178, CD-ROM, pp. 1–33. Available from: Ocean Drilling Program, College Station, TX, 77845-9547, USA.
Hillenbrand, C.-D., Ehrmann, W., 2005. Late Neogene to Quaternary environmental change in the Antarctic Peninsula region: evidence from drift sediments. Global and Planetary Change 45, 165–191.
Hovan, S.A., 1995. Late Cenozoic atmospheric circulation intensity and climate history recorded by eolian deposition in the eastern equatorial Pacific Ocean, Leg 138. In: Pisias, N.G., Mayer, L.A., Janecek, T.R., Palmer-Julson, A., van Andel, T.H. (Eds.), Proceedings of the Ocean Drilling Program, Scientific Results, Leg 138, pp. 615–625.
Joseph, L.H., Rea, D.K., van der Pluijm, B.A., 1998. Use of grain size and magnetic fabric analyses to distinguish among depositional environments. Paleoceanography 13, 491–501.
Joseph, L.H., Rea, D.K., van der Pluijm, B.A., Gleason, J.D., 2002. Antarctic environmental variability since the late Miocene: ODP Site 745, the East Kerguelen sediment drift. Earth and Planetary Science Letters 201, 127–142.
Joseph, L.H., Rea, D.K., van der Pluijm, B.A., 2004. Neogene history of the Deep Western Boundary Current at Rekohu sediment drift, Southwest Pacific (ODP Site 1124). Marine Geology 205, 185–206.
Kerr, B.C., Scholl, D.W., Klemperer, S.L, 2005. Seismic stratigraphy of Detroit Seamount, Hawaiian-Emperor seamount chain: post-hot-spot shield-building volcanism and deposition of the Meiji drift. Geochemistry, Geophysics, Geosystems 6 (7). doi:10.1029/2004GC000705 Q07L10.
Kidd, R.B., Hill, P.R., 1987. Sedimentation on Feni and Gardar sediment drifts. In: Ruddiman, W.F., Kidd, R.B., Thomas E. (Eds.), pp. 1217–1244. Init. Repts. DSDP, 94, Washington.
Lawver, L.A., Gahagan, L.M., 2003. Evolution of Cenozoic seaways in the circum-Antarctic region. Palaeogeography, Palaeoclimatology, Palaeoecology 198, 11–37.
Ledbetter, M.T., 1979. Fluctuations of Antarctic Bottom Water velocity in the Vema Channel during the last 160,000 years. Marine Geology 33, 71–89.
Ledbetter, M.T., 1984. Bottom-current speed in the Vema channel recorded by particle size of sediment fine-fraction. Marine Geology 58, 137–149.
Ledbetter, M.T., Ellwood, B.B., 1980. Spatial and temporal changes in bottom-water velocity and direction from analysis of particle size and alignment in deep-sea sediment. Marine Geology 38, 245–261.
Lyle, M., Gibbs, S., Moore, T.C., Rea, D.K., 2007. Late Oligocene initiation of the Antarctic Circumpolar Current: evidence from the South Pacific. Geology 35, 691–694. doi:10.1130/23806A.1.
Maldonado, A., et al., 2003. Contourite deposits in the central Scotia Sea: the importance of the Antarctic Circumpolar Current and the Weddell Gyre flows. Palaeogeography, Palaeoclimatology, Palaeoecology 198, 187–221.
Maldonado, A., et al., 2005. Miocene to Recent contourite drifts development in the northern Weddell Sea (Antarctica). Global and Planetary Change 45, 99–129.
Maslin, M.A., Haug, G.H., Sarnthein, M., 1996. The progressive intensification of northern hemisphere glaciation as seen from the North Pacific. Geol Rundsch 85, 452–465.
Maslin, M.A., Li, X.S., Loutre, M.F., Berger, A., 1998. The contribution of orbital forcing to the progressive intensification of Northern Hemisphere Glaciation. Quaternary Science Reviews 17, 411–426.
McCave, I.N., Manighetti, B., Beveridge, N.A.S., 1995. Circulation in the glacial North Atlantic inferred from grain-size measurements. Nature 374 (6518), 149–152.
Naish, T., et al., 2009. Obliquity-paced Pliocene West Antarctic ice sheet oscillation. Nature 458, 322–329. doi:10.1038/nature07867.
Orsi, A.H., Whitworth III, T., Nowlin Jr, W.D., 1995. On the meridional extent and fronts of the Antarctic Circumpolar Current. Deep-Sea Research I 42 (5), 641–673.
Naveira Garabato, A.C., Polzin, K.L., King, B.A., Heywood, K.J., Visbeck, M., 2004. Widespread intense turbulent mixing in the Southern Ocean. Science 303, 210–213.
Parés, J.M., van der Pluijm, B.A., 2002. Phyllosilicate fabric characterization by low-temperature anisotropy of magnetic susceptibility (LT-AMS). Geophysical Research Letters 29. doi:10.1029/2002GL015459,2002.
Parés, J.M., Hassold, N.J.C., Rea, D.K., van der Pluijm, B.A., 2007. Paleocurrent directions from paleomagnetic reorientation of magnetic fabrics in deep-sea sediments at the Antarctic Peninsula Pacific margin (ODP Sites 1095, 1101). Marine Geology 242, 261–269. doi:10.1016/j.margeo.2007.04.002.
Pfuhl, H.A., McCave, I.N., 2005. Evidence for late Oligocene establishment of the Antarctic Circumpolar Current. Earth and Planetary Science Letters 235, 715–728.
Pudsey, C.J., 2001. Data report: grain-size data, sites 1095, 1096, and 1101, Antarctic Peninsula continental rise. In: Barker, P.F., Camerlenghi, A., Acton, G.D., Ramsay, A.T.S. (Eds.), CD-ROM, pp. 1–34. Available from: Ocean Drilling Program, College Station, TX, 77845-9547, USA.
Pudsey, C.J., Howe, J.A., 1998. Quaternary history of the Antarctic Circumpolar Current: evidence from the Scotia Sea. Marine Geology 148, 83–112.
Ravelo, A.C., Andreasen, D.H., 2000. Enhanced circulation during a warm period. Geophysical Research Letters 27, 1001–1004.
Raymo, M.E., Hodell, D., Jansen, E., 1992. Response of deep ocean circulation to initiation of Northern Hemisphere Glaciation (3–2 Ma). Paleoceanography 7, 645–672.
Rea, D.K., Hovan, S.A., 1995. Grain size distribution and depositional processes of the mineral component of abyssal sediments: lessons from the North Pacific. Paleoceanography 10, 251–258.
Rea, D.K., Snoeckx, H., 1995. Sediment fluxes in the Gulf of Alaska: paleoceanographic record from Site 887 on the Patton–Murray Seamount platform. In: Rea, D.K., Basov, I.A., Scholl, D.W., Allan, J.F. (Eds.), Proceedings of the Ocean Drilling Program, Scientific Results, 145. Ocean Drilling Program, College Station, TX, pp. 247–256.
Rea, D.K., Janecek, T.R., 1981. Mass-accumulation rates of the non-authigenic inorganic crystalline (eolian) component of deep-sea sediments from the western mid-Pacific mountains, Deep Sea Drilling Project Site 463. In: Thiede, J., Vallier, T.L., et al. (Eds.), Initial Reports of the Deep Sea Drilling Project, pp. 653–659.
Rebesco, M., Camerlenghi, A., 2008. Late Pliocene margin development and mega debris flow deposits on the Antarctic continental margins: evidence of the onset of the modern Antarctic Ice Sheet? Palaeogeography, Palaeoclimatology, Palaeoecology 260, 149–167. doi:10.1016/j.palaeo.2007.08.009.
Rebesco, M., Camerlenghi, A., Geletti, R., Canals, M., 2006. Margin architecture reveals the transition to the modern Antarctic ice sheet ca. 3 Ma. Geology 34 (4), 301–304.
Rebesco, M., Larter, R.D., Barker, P.F., Camerlenghi, A., Vanneste, L.E., 1997. The history of sedimentation on the continental rise west of the Antarctic Peninsula. In: Barker, P.F., Cooper, A.K. (Eds.), Geology and Seismic Stratigraphy of the Antarctic Margin (Pt. 2). Am. Geophys. Union, Antarctic Res. Ser., pp. 20–50.
Rees, A.I., Woodall, W.A., 1975. The magnetic fabric of some laboratory-deposited sediments. Earth and Planetary Science Letters 25, 121–130.
Richter, C., van der Pluijm, B.A., 1994. Separation of paramagnetic and ferrimagnetic susceptibilities and comparison with high field methods. Physics of the Earth and Planetary Interiors 82, 113–123.
Sigman, D.M., Jaccard, S.L., Haug, G.H., 2004. Polar ocean stratification in a cold climate. Nature 428, 59–63.
Tarling, D.H., Hrouda, F., 1993. The Magnetic Anisotropy of Rocks. Chapman and Hall, New York. 217 pp.
Uenzelmann-Neben, G., 2006. Depositional patterns at Drift 7, Antarctic Peninsula: along-slope versus down-slope sediment transport as indicators for oceanic currents and climatic conditions. Marine Geology 233, 49–62. doi:10.1016/j.margeo.2006.08.008.
van de Flierdt, T., et al., 2004. Deep and bottom water export from the Southern Ocean to the Pacific over the past 38 million years. Paleoceanography 19. doi:10.1029/2003PA000923,2004 PA1020.
Wright, J.D., Miller, K.G., Fairbanks, R.G., 1991. Evolution of modern deepwater circulation: evidence from the late Miocene Southern Ocean. Paleoceanography 6, 275–290.